

Group Convolutional Neural Networks Improve Quantum State Accuracy

Christopher Roth and Allan H. MacDonald
Physics Department, University of Texas at Austin

Neural networks are a promising tool for simulating quantum many body systems. Recently, it has been shown that neural network-based models describe quantum many body systems more accurately when they are constrained to have the correct symmetry properties. In this paper, we show how to create maximally expressive models for quantum states with specific symmetry properties by drawing on literature from the machine learning community. We implement group equivariant convolutional networks (G-CNN) [1], and demonstrate that performance improvements can be achieved without increasing memory use. We show that G-CNNs achieve very good accuracy for Heisenberg quantum spin models in both ordered and spin liquid regimes, and improve the ground state accuracy on the triangular lattice over other variational Monte-Carlo methods.

I. INTRODUCTION

Because quantum physics problems with interacting degrees of freedom grow exponentially with the number of degrees of freedom, accurate numerical solutions are often available only for relatively small system sizes. Simulations nevertheless play a valuable role in advancing understanding because they have the important advantages over experiments on real physical systems that the problem being solved is fully characterized and free from unintended disorder. Neural network quantum states (NQS) ([2–9]) have emerged as a competitive tool for understanding the low temperature properties of quantum many-body physics models. Unlike traditional variational Monte-Carlo (VMC) methods, such as Gutzwiller projection, neural networks have the advantage, and also the disadvantage, of being free from inductive biases about the structure of the solution. They compensate for the absence of an informed bias by using an enormous number of parameters. As long as a wide enough model is used, neural networks contain arbitrarily accurate solutions [10].

Although reasonably large neural networks are guaranteed to harbor good solutions in the space of possible parameters, there is no guarantee that these solutions can be found in a reasonable time. One way to accelerate training is to constrain the search space by removing non-solutions. This is especially useful on lattice problems which have highly symmetric low-lying energy levels. Recent research [7, 11–15] has shown that forcing neural networks to have the correct symmetry tremendously improves their ability to model the ground state and low-lying excited states of quantum many-body systems.

Other research in the field of NQS has focused on training deeper models, specifically convolutional neural networks (CNN) [8, 11, 16]. This is motivated by the field of computer vision [17, 18], in which deep convolutional neural networks have excelled at pattern recognition. While both images and quantum ground states often have translational symmetry, quantum ground states frequently have additional point group symmetry. In this paper we leverage literature from the machine learning

community [1] to generalize convolutional NQS to the full wallpaper group of highly symmetric lattices.

We show that group equivariant convolutional networks (G-CNN) [1] provide the most expressive perceptron-like model for wavefunctions with particular symmetry over discrete groups. G-CNNs are constructed using equivariant convolutions, which are the most complex linear operations that preserve the structure of a discrete symmetry group [1]. This approach contrasts with previous research [7, 11, 12], which has utilized a symmetry-averaging procedure in which the model is applied to symmetry-transformations of the input and the output is averaged. We show that G-CNNs can be mapped to symmetry-averaged linear models by zeroing out some filters between hidden layers. When we mask a G-CNN in this manner, *i.e.* when we constrain it to match previous symmetry-averaging procedures, the performance degrades.

We use a G-CNN with local translational filters to simulate frustrated $J_1 - J_2$ Heisenberg models on square and triangular lattices. Both of these Hamiltonians give rise to rich phase diagrams that include magnetically ordered states and spin liquid states that do not order but have non-trivial quantum entanglement. Our model gives accurate results for both triangular and square lattice phase-diagrams, and compares favorably with state-of-the-art variational Monte-Carlo (VMC) results on the triangular lattice.

II. VMC WITH NEURAL NETWORK QUANTUM STATES

We compute ground state energies for the frustrated $J_1 - J_2$ Heisenberg model on the square and triangular lattices. The Hamiltonian is given by:

$$H = J_1 \sum_{i,j \in \langle \rangle} \sigma_i \cdot \sigma_j + J_2 \sum_{i,j \in \langle \langle \rangle \rangle} \sigma_i \cdot \sigma_j, \quad (1)$$

where $\langle \rangle$ and $\langle \langle \rangle \rangle$ are nearest and next-nearest neighbor links and $J_1, J_2 > 0$. We use a neural-network ansatz that associates a complex number $\psi(\sigma)$ with each config-

uration of spins σ . These define the wavefunction:

$$|\psi\rangle = \sum_{\sigma} \psi(\sigma) |\sigma\rangle. \quad (2)$$

We optimize our Ansatz using gradient based methods as detailed in Carleo *et al.* [2].

III. SYMMETRIC NEURAL NETWORK WAVEFUNCTIONS

Symmetry-averaging neural networks has been shown to improve performance in both machine learning applications [1, 19–22] and quantum many-body VMC applications [12, 23, 24]. Below, we first discuss symmetry-averaging from the point of view of equivariance. We then show that that G-CNNs provide a richer model class, which can be mapped down to symmetry-averaged models by masking filters.

A. The Principle of Equivariance

An equivariant function acts on a G-space [1, 25], a set of objects, S , that are related by the symmetry transformations of a group, G . In this paper we consider the set of transformations, generated by lattice translations and the d4(6) point group for square (triangular) lattices. These are the groups of transformations that leave the lattices unchanged. An equivariant function is one that transforms a G-set of poses while preserving the group structure,

$$g' \mathcal{F}(\{\mathbf{f}\}_S) = \mathcal{F}(g\{\mathbf{f}\}_S), \quad (3)$$

where $\{\mathbf{f}\}_S$ is a set of features over the set S . Here g' and g do not be the same operator, but they must be generators of isomorphic groups. For example if $g = T_{x,y}$ is a translation on a periodic 2D square lattice of length L , then $g' = T_{x',y'}$ must also be a translation that is cyclic over L in both dimensions.

B. Symmetry-Averaged Models are Equivariant Models

Symmetry can be imposed [24] on a model wavefunction ψ by a symmetry-averaging procedure that applies the model to all symmetry-transformations of the input and performs a phase-factor weighted average over outputs:

$$\psi(\sigma) = \sum_g \chi_g \tilde{\psi}(g^{-1}\sigma). \quad (4)$$

Here χ_g is the character of symmetry operation g , and g^{-1} is the inverse of g , which means that $gg^{-1} = g^{-1}g = I$. This procedure can also be thought of as averaging

over the output of an equivariant model $\psi_g(\sigma)$ if we define:

$$\psi_g(\sigma) = \tilde{\psi}(g^{-1}\sigma). \quad (5)$$

This definition recasts a single model $\tilde{\psi}$ applied to N_G inputs, as an equivariant model ψ_g with output dimension N_G applied to a single input. Note that a symmetry transformation on the input to ψ_g yields a symmetry operation on the output:

$$\psi_g(u^{-1}\sigma) = \tilde{\psi}(g^{-1}u^{-1}\sigma) = \psi_{ug}(\sigma). \quad (6)$$

We see that is still equivariant, as the set of transformations $\{u\}$ and $\{u^{-1}\}$ form isomorphic groups. Using this new definition, the symmetrization procedure expresses the wavefunction as follows:

$$\psi(\sigma) = \sum_g \chi_g \psi_g(\sigma). \quad (7)$$

This still produces a ψ that has the desired character:

$$\begin{aligned} \psi(u\sigma) &= \sum_g \chi_g \psi_g(u\sigma) = \sum_g \chi_g \psi_{u^{-1}g}(\sigma) \\ &= \sum_g \chi_{ug} \psi_g(\sigma) = \sum_g \chi_u \chi_g \psi_g(\sigma) = \chi_u \psi(\sigma). \end{aligned} \quad (8)$$

From this discussion we see that symmetry-averaging is not required to restrict symmetry eigenvalues. Only equivariance is needed. In this paper, we replace the symmetry averaging procedure by a G-CNN, which consists of stacked equivariant convolutional layers [1] interspersed with non-linearities. The G-CNN architecture allows us to scale up the number of parameters without using more memory, and improves performance on difficult optimization problems.

C. Generalizing Translational Convolutions to Discrete Groups

Equivariance under the translational group is present in standard convolutional neural networks (CNNs),

$$C_{x,y}^i = \sum_{x',y' < L} \mathbf{W}_{x'-x,y'-y}^i \cdot \mathbf{f}_{x',y'}, \quad (9)$$

that satisfy periodic boundary conditions. The filters $\mathbf{W}_{x'-x,y'-y}^i$ look at patterns in the feature map $\mathbf{f}_{x',y'}$ separated from x, y by $\{x' - x, y' - y\}$. CNNs work by alternating convolution operations with non-linearities to develop increasingly abstract representations of the input.

The G-CNN generalizes the CNN to act over a discrete group G , which may contain non-commuting operations. For our implementation, we consider the full wallpaper group, which adds rotation and mirror symmetry on top of translation. The group convolution operation is written as follows:

$$C_g^i = \sum_{h \in G} \mathbf{W}_{g^{-1}h}^i \cdot \mathbf{f}_h. \quad (10)$$

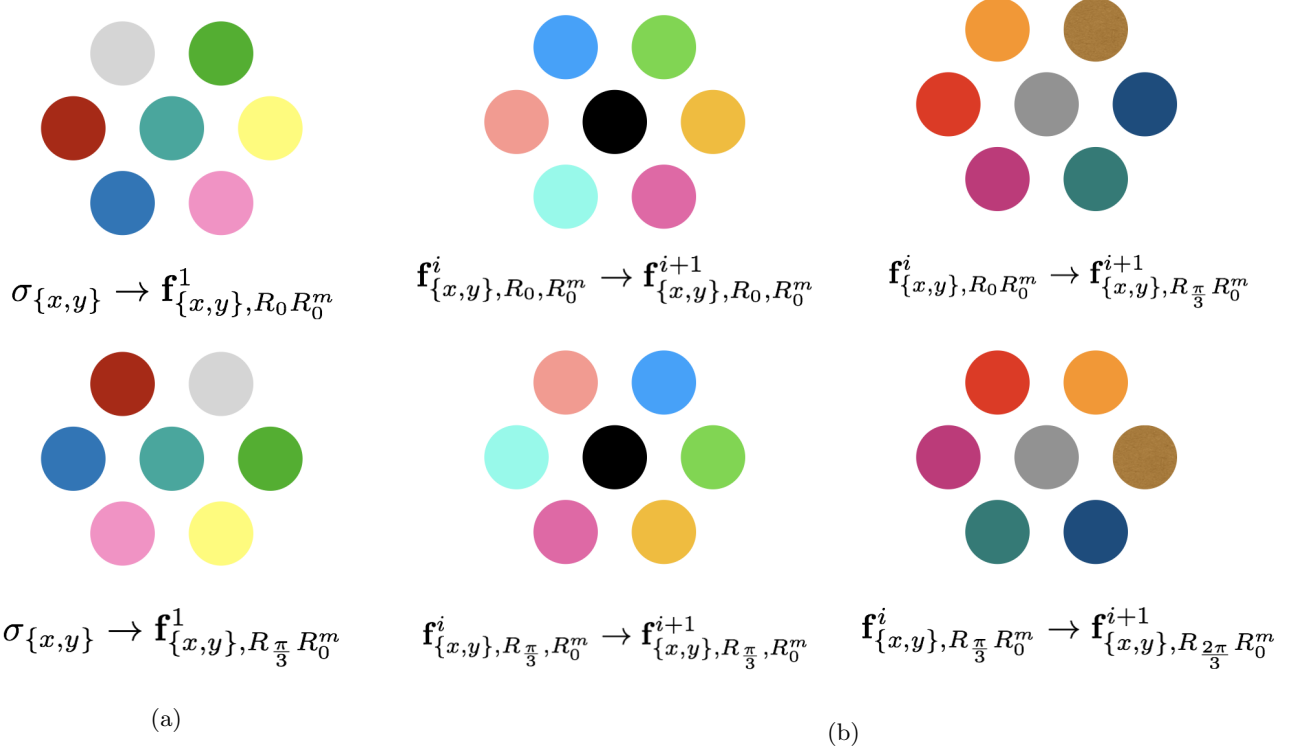


FIG. 1: Schematic of an equivariant convolutional model on a triangular lattice with p6m symmetry. Nearest neighbor convolutions are drawn for legibility. a) Equivariant convolution connecting the input to the feature maps. Each feature map uses a set of filters with a specified symmetry transformation over d_6 . (b) Equivariant convolution connecting feature maps at adjacent layers. There are 12 sets of filters that connect poses based on their relative orientations.

For the G-CNN, the feature map is defined over the G-space generated by the wallpaper group, instead of just the translation group. We see that the group convolution is equivariant, since a group operation on input yields the same group operation on the output:

$$\sum_{h \in G} \mathbf{W}_{g^{-1}h}^i \cdot \mathbf{f}_{uh} = \sum_{h \in G} \mathbf{W}_{g^{-1}u^{-1}h}^i \cdot \mathbf{f}_h = C_{ug}^i. \quad (11)$$

This linear operation is the building block of our model.

D. Our Model

We use a model that is similar to a G-CNN [1], and specified by a stack of equivariant convolutional layers interspersed with pointwise non-linearities. The first convolution takes the z-components of the spins, σ_x , where x are the lattice site labels, and outputs a feature map over the full wallpaper group:

$$\mathbf{f}_g^1 = \Gamma \left(\sum_x W_{g^{-1}x}^0 \sigma_x \right), \quad (12)$$

where Γ is a point-wise non-linearity. This convolution is diagrammed in Fig. 1a. The feature-to-feature convo-

lutions are performed as in equation 10:

$$\mathbf{f}_g^{i+1} = \Gamma \left(\sum_{h \in G} W_{g^{-1}h}^i \mathbf{f}_h^i \right). \quad (13)$$

The structure of these convolutions is seen in Fig. 1b. We compute our wavefunction with character $\{\chi_g\}$ by phase-weighting over the exponential our final embedding, f_g^N , which has length one:

$$\psi(\sigma) = \sum_g \chi_{g^{-1}} \exp(f_g^N). \quad (14)$$

We choose Γ to be the SELU nonlinearity [26] applied separately to the real and imaginary parts,

$$\Gamma(x) = \text{SELU}(\text{Re}(x)) + i\text{SELU}(\text{Im}(x)). \quad (15)$$

The SELU nonlinearity moves the distribution of activations in the direction of zero mean and one variance, which enables stable training of deep networks. We note that for all models studied in this paper, the ground state is fully symmetric, i.e. $\chi_g = 1$ for all g .

While this model may appear complicated, we believe it is actually quite simple. It is just a multi-layer perceptron, with alternating linear and pointwise non-linear transformations, in which weights are tied together to

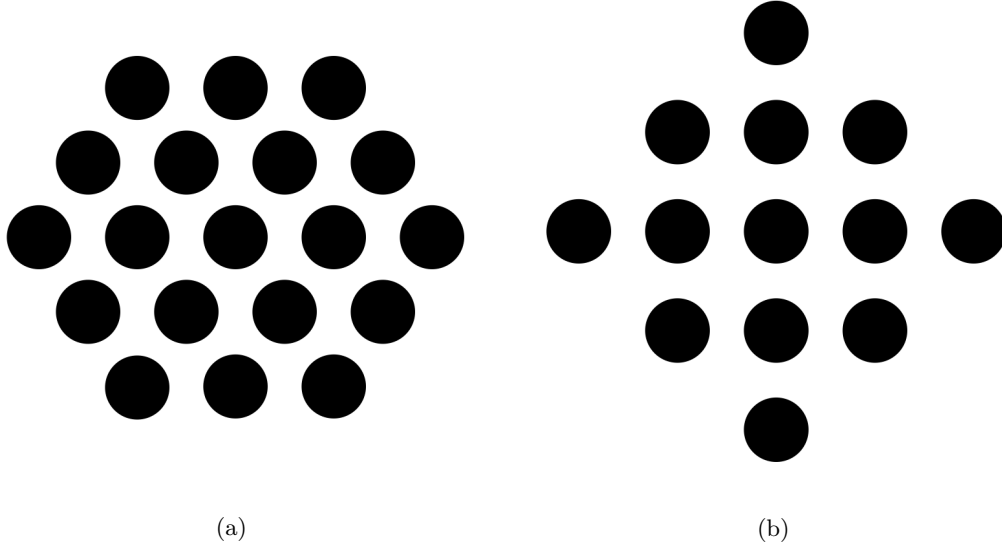


FIG. 2: Filter shapes for our restricted equivariant convolution operation on the a) triangular lattice (b) square lattice. For both lattices, interactions are restricted to third nearest neighbors.

force particular symmetry properties. Training a simple model, with a constant feature dimension and with neither bells nor whistles, will demonstrate the power of this approach.

IV. RESULTS

We begin by showing results from our best performing model, which uses a G-CNN architecture with local filters. This model achieves state-of-the-art VMC ground state energies on the triangular lattice, and competitive energies on the square lattice. We then examine how the performance of the G-CNN is affected by masking off-diagonal filters. As detailed in section VIII B, this simplification maps G-CNNs to models that are forced to be equivariant by symmetry-averaging. The optimization details for both of these experiments are outlined in section VIII E.

A. Results from our Best Performing Model

In Table I we summarize a variety of ground state energy estimates obtained using different methods for 6×6 finite-size J_1, J_2 triangular lattice Heisenberg models. For this lattice size, the DMRG[27] and ED[28] estimates agree to five figures and are essentially exact. For the $J_2 = 0$ case our model achieves $\sim 0.2\%$ accuracy for the energy, compared to the $\sim 1\%$ accuracy achieved by other variational methods in the literature. For $J_2 = J_1/8$, in the spin-liquid regime, the ground state energy error is reduced by a factor of ~ 3 compared to literature VMC estimates. VMC calculations often add

Lanczos steps [29] to improve variational energy accuracies; our ground state energies surpasses all other VMC methods in accuracy even without this elaboration.

	$J_2 = 0$	$J_2 = J_1/8$
ED [28]	-0.5603734	-0.515564
DMRG [27]	-0.560375	-0.51557
G-CNN	-0.55922	-0.51365
NN + Gutzwiller [12]	-0.553	N/A
VMC + 2LS [27]	N/A	-0.512503
VMC [30]	-0.55519	-0.5089
VMC [31]	-0.55420	N/A
VMC [27]	-0.548025	-0.501788

TABLE I: Comparison between finite size 6×6 triangular lattice ground state energies estimates

We studied the dependence of performance, measured by the accuracy of ground state energy estimates, on the range of the filter for $J_2 = J_1/8$. Restricting the connectivity reduces computational overhead, and biases the model towards learning short range interactions. Changing the filter shape changes the way in which the model conveys information about the connectivity of the lattice. We tried a few different symmetric filter shapes and settled on a version that convolves over third-nearest-neighbors, as shown in Fig. 2.

In order to demonstrate the robustness of our model, we applied the same architecture to the ordered and spin liquid regimes of the square lattice $J_1 - J_2$ Heisenberg model. Remarkably, across all four domains, we only had to adjust a single learning rate. The results on the square lattice are summarized in Table II

We make a direct comparison to the square lattice CNN model described in Choo et al. [11] who use a

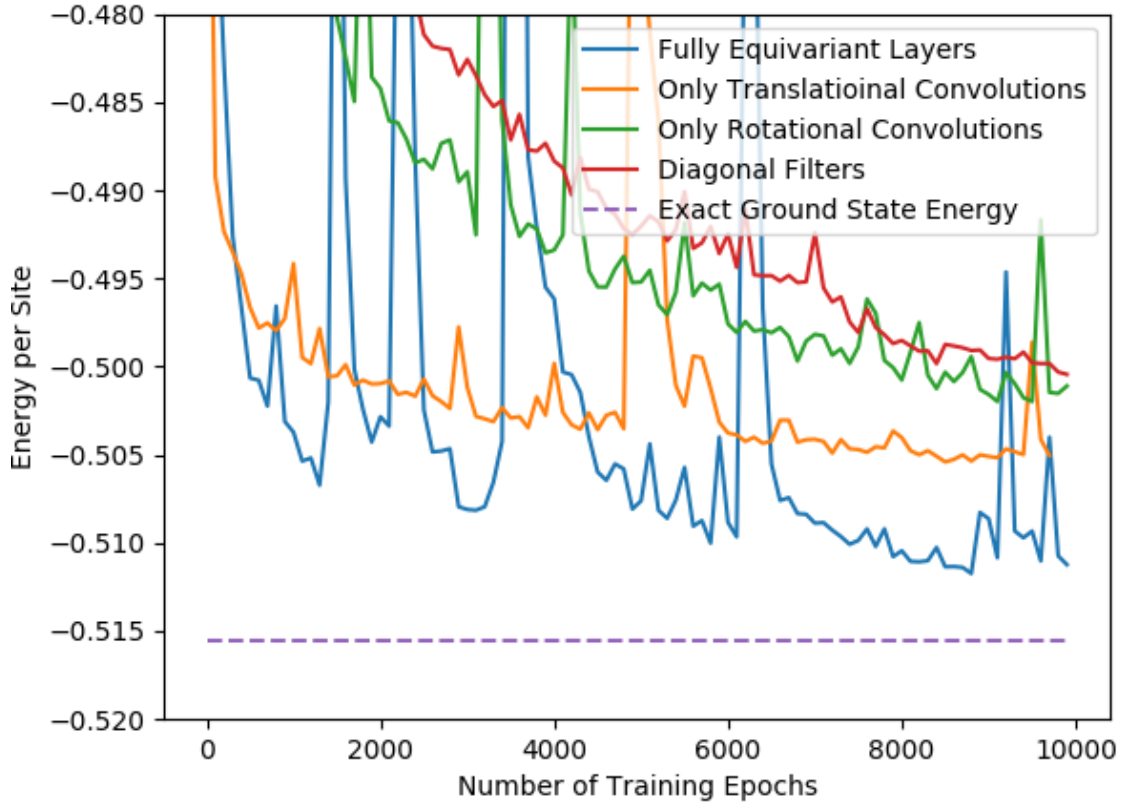


FIG. 3: Performance of the G-CNN on the triangular Heisenberg model ($J_2 = \frac{1}{8}$) as various off-diagonal filters are set to zero. As described in section VIII B this is equivalent to replacing group convolution with symmetry averaging. All models are trained using the Adam optimizer with a learning rate of 3×10^{-3}

	G-CNN	CNN + c_4	RBM + PP
$J_2 = J_1/2$	0.17%	0.39%	0.022%
$J_2 = 0$	0.016%	0.007%	N/A
Max Memory	$16 \times N_g$	$10 \times N_g$	$576 \times N_g$
N_{params}	113360	3838	22032

TABLE II: Errors relative to exact diagonalization for 6×6 square-lattice finite-size ground state states. The number of variational parameters and the memory usage are compared for different approaches.

translationally equivariant CNN symmetry-averaged over c_4 , while we use a model that is equivariant over the full space group $p4m$. As explained in section VIII B of the appendix, their model can be mapped to a G-CNN over $p4$ with masked off-diagonal rotational filters. Our model uses slightly more memory, while their model has more layers and uses an improved optimizer. We see that the G-CNN model nevertheless has better ground state energy accuracy on the difficult-to-simulate spin-liquid state. Neither CNN architecture is competitive with the

architecture detailed by Nomura et al. [7], who combine a restricted Boltzmann machine with a pair product state (RBM+PP). Theirs is a shallower model that uses far more memory. For the ordered state, both CNN based methods are very accurate, and the discrepancy may be due to convergence issues [32] with the adaptive moment (Adam) parameter optimizer [33].

We note that the equivariant model has by far the best parameter-number to memory ratio, as it adds connectivity along the entire d_4 symmetry group. Maximizing the number of parameters in a memory profile [34, 35] is important for performance improvement on massively parallel modern hardware. Even though our model has more parameters than the RBM + PP model, it is likely much faster to train on a GPU.

B. Effect of Off-Diagonal Filters

We document the importance of full connectivity using the $J_1 - J_2$ Heisenberg model on a triangular lattice with $J_2 = J_1/8$. This is a difficult system to simulate

since it gives rise to a spin liquid state with no magnetic order and non-trivial entanglement. We train four models with different feature-to-feature connectivities to test the effect of replacing layer-wise equivariance with symmetry averaging. We do this by applying a masking procedure, where we set off-diagonal filters to zero. Here, the term off-diagonal distinguishes between filters that connect poses of the same orientation in a particular symmetry group and filters that connect different orientations. As an example, filters in equation 9 with $\{x', y'\} = \{x, y\}$ are translationally diagonal whereas all others are translationally off-diagonal.

First we train a model with diagonal feature-to-feature interactions along all groups, corresponding to a fully connected linear model symmetrized over $p6m$. Second we train models with off-diagonal features in translation and rotation set to zero. These correspond to models that convolve over some degrees of freedom, and symmetry average over others. Finally, we compare all of these with a G-CNN with full connectivity. While all four of these models use the same amount of memory, they have vastly different numbers of parameters.

Connectivity	Full	Translational	d_6	Diagonal
N_{params}	449856	38016	13056	1616

TABLE III: Comparison between the number of parameters of different equivariant architectures

We see in Fig. 3 that adding a richer layer structure systematically improves the performance. The model with fully-connected layers markedly outperforms the others, surpassing their performance in 1/10 of the training time. We also see in Fig. 3 that the energy estimates are not monotonic functions of training time. This behavior is related to our use of high learning rates that enable escapes from local minima. Although higher learning rates worsen the performance temporarily, we find that the final variational energies are ultimately superior.

We see that translational filters have a bigger effect on performance than rotational filters. This could simply be due to the number of parameters in the models. On a 6×6 lattice, adding translational interactions increases the number of parameters by a factor of 36, while adding d_6 interactions only increases the number of parameters by a factor of 12.

V. DISCUSSION AND CONCLUSION

In this paper we use a G-CNN to find the ground wavefunction of the frustrated Heisenberg model on the square and triangular lattices. We find that the G-CNN architecture yields accurate ground state energies for both magnetically ordered states and spin liquids, including the most accurate VMC energies on the triangular lattice to date.

Among perceptron-like models, G-CNN models are more expressive than symmetry-averaged models. We explicitly demonstrate how performance degrades as the model class is constrained. For the wallpaper group $p6m$, we see that it is important to convolve over both translation operations and the point group.

For our experiments we used the simplest kind of neural network model that satisfies the symmetry constraints, a multi-layer perceptron with tied weights. We note that other advances in machine learning, such as depthwise convolutions [36] and attention [37], can also be implemented with group equivariance [38]. Implementing these models could certainly further improve the performance of the quantum spin model ground state calculations we have discussed, and other quantum ground state calculations. Although we only studied relatively small systems, these calculations could be scaled to larger systems by combining sparsification, transfer learning, and efficient sampling [39].

Finally, we note that several other papers have studied the importance of using equivariant models applied to different symmetry groups. Luo *et al.* [14] show that gauge equivariant neural networks improve performance on gauge invariant Hamiltonians [13], and Pfau *et al* [40] use a permutation equivariant model to account for identical electrons. Since many important physics models have substantial symmetry, applications of equivariant models are likely to be important for machine-learning methods in computational physics.

VI. CODE

Code for implementing G-CNNs on NQS will be made publically available through NetKet [41] in the near future. Pytorch code for these experiments will be uploaded at <https://github.com/chrisrothUT/>

VII. ACKNOWLEDGEMENTS

Chris Roth acknowledges helpful interactions with Mohamed Hibat-Allah, Juan Carrasquilla and Giuseppe Carleo. This work was supported in part by the Army Research Office (ARO) Grant # W911NF-17-1-0312 (MURI).

VIII. APPENDIX

A. Implementation of the Equivariant Convolution

We implement our equivariant convolution exactly as in Cohen *et al.* [1]. We learn an index mapping that relates our filters of shape $[d_{in}, d_{out}, N_g]$ to a group of 2D convolutions with rotated filters as depicted in 1b. Then we concatenate the rotation/reflection with the channel

dimension and apply a 2D convolution. For details see the aforementioned paper.

B. Equivariant Models can be Mapped to other Symmetrized models by Constraining Filters

Recently several groups [7, 8, 11, 12, 42] have accurately simulated the frustrated $J_1 - J_2$ Heisenberg model on a square lattice by constraining the symmetry eigenvalues. While some of these models used translational convolutions, none of them convolved over the entire wallpaper group $p4m$ as done by the G-CNN.

We demonstrate how the G-CNN can be mapped down to other multi-layer linear models by masking filters. For the sake of brevity, we show the mapping between the $p4m$ G-CNN and a) a linear model symmetry-averaged over $p4m$ b) a translationally equivariant model symmetry averaged over d_4 .

We construct a symmetry operation in $p4m$ by first applying a reflection, followed by a rotation and a translation,

$$S_{x,y,\alpha,\beta} = T_{xy}R_\alpha R_\beta^m. \quad (16)$$

Using equation 10, we can write the filter that connects two G-set elements in neighboring layers.

$$S_{x,y,\alpha,\beta}^{-1} S_{x',y',\alpha',\beta'} = R_{-\beta}^m R_{-\alpha} T_{x'-x,y'-y} R_{\alpha'} R_{\beta'}^m. \quad (17)$$

This is a convolution operation with filters transformed by $p4m$ as shown in Fig. 1b.

To map to a multi-layer linear model symmetry-averaged over $p4m$, the input-to-feature filters are kept the same and the feature-to-feature filters are restricted to be diagonal, $\alpha = \alpha'$, $\beta = \beta'$, $x = x'$ and $y = y'$.

The new feature-to-feature convolution becomes

$$\mathbf{f}_{x,y,\alpha,\beta}^{i+1} = \sigma(W^i \mathbf{f}_{x,y,\alpha,\beta}^i). \quad (18)$$

This is equivalent to applying the same linear model to each pose. The different poses are generated by the symmetry transformed filters shown in Fig. 1a. Equivalently, we could generate the poses by symmetry transforming the input and keeping the filters the same. As a result, we see that the G-CNN with diagonal feature-to-feature filters is equivalent to a linear model symmetrized over $p4m$.

We can also map the G-CNN to a translationally equivariant model (CNN) symmetrized over d_4 by constraining $\alpha = \alpha'$ and $\beta = \beta'$. With this constraint the feature-to-feature convolution is

$$\mathbf{f}_{x,y,\alpha,\beta}^{i+1} = \sum_{x',y'} \sigma(W_{x'-x,y'-y,\alpha,\beta}^i \mathbf{f}_{x',y',\alpha,\beta}^i). \quad (19)$$

The feature-to-feature convolution now consists of CNNs applied to each pose in d_4 labeled by α, β where the filters of each CNN are transformed according to the group

element

$$W_{x'-x,y'-y,\alpha,\beta}^i = R_{-\beta}^m R_{-\alpha} W_{x'-x,y'-y}^i R_\alpha R_\beta^m \quad (20)$$

Again, if we change basis and transform the input instead of the filters, this is a CNN symmetrized over d_4 . Both of these examples show that symmetry-averaging creates a more restrictive model class than the G-CNN for multi-layer networks.

C. Triangular Heisenberg on a Rectangular Grid

We implement the triangular Heisenberg model on a rectangular graph by noting that a triangular graph is isometric to a rectangular graph with coupling along one of the diagonals. We implement our models on 6×6 tori with periodic boundary conditions (PBCs) and coupling along one of the diagonals. This is equivalent to a hexagonal shaped lattice with 36 sites.

D. Coordinate Mappings

On the square lattice, a $\frac{\pi}{2}$ rotation is defined by the coordinate mapping $(i, j) \rightarrow (-j, i)$ where the coordinates are defined modulo L. On the triangular lattice a $\frac{\pi}{3}$ mapping is accomplished by a coordinate mapping $(i, j) \rightarrow (i - j, i)$. We can arbitrarily choose a reflection axis, and for simplicity we do the coordinate transform $(i, j) \rightarrow (j, i)$ for both geometries.

E. Optimization Details

Our best performing model had 4 layers and 16 hidden nodes. We used the Adam optimizer [33] with a learning rate of 3×10^{-3} and the default parameters. We optimized our learning rate and network architecture on the triangular lattice with $J_2 = 0.125$ and used the same hyperparameters for the other systems, except for the square lattice with $J_2 = 0$ where we found that the learning rate was too high, and decreased it by a factor of 3.

Our optimization procedure was as follows. First, we optimized the phase structure for 500 steps by setting $Re(\log(\psi)) = 0$ before outputting ψ . We found that pre-optimizing the phases [42], which helps avoid local-minima, was crucial to successfully finding the ground state. We then trained both amplitudes and phases for 10^4 steps at batch size 100 before increasing the batch size to 1000 and training for an additional 2×10^3 steps.

We tuned the learning rate (on the triangular lattice at $J_2 = \frac{1}{8}$) by altering it by factors of 3 and modified N_{hidden} and N_{layers} under the constraint $N_{hidden} \times N_{layers} = 64$. We found that a ratio of $\frac{N_{hidden}}{N_{layers}} = 4$ worked best.

-
- [1] Taco Cohen and Max Welling. Group equivariant convolutional networks. In *International conference on machine learning*, pages 2990–2999. PMLR, 2016.
- [2] Giuseppe Carleo and Matthias Troyer. Solving the quantum many-body problem with artificial neural networks. *Science*, 355(6325):602–606, 2017.
- [3] Juan Carrasquilla. Machine learning for quantum matter. *Advances in Physics: X*, 5(1):1797528, 2020.
- [4] Or Sharir, Yoav Levine, Noam Wies, Giuseppe Carleo, and Amnon Shashua. Deep autoregressive models for the efficient variational simulation of many-body quantum systems. *Physical review letters*, 124(2):020503, 2020.
- [5] Mohamed Hibat-Allah, Martin Ganahl, Lauren E Hayward, Roger G Melko, and Juan Carrasquilla. Recurrent neural network wave functions. *Physical Review Research*, 2(2):023358, 2020.
- [6] Christopher Roth. Iterative retraining of quantum spin models using recurrent neural networks. *arXiv preprint arXiv:2003.06228*, 2020.
- [7] Yusuke Nomura and Masatoshi Imada. Dirac-type nodal spin liquid revealed by machine learning. *arXiv preprint arXiv:2005.14142*, 2020.
- [8] Xiao Liang, Shao-Jun Dong, and Lixin He. Hybrid convolutional neural network and projected entangled pair states wave functions for quantum many-particle states. *Physical Review B*, 103(3):035138, 2021.
- [9] Nikita Astrakhantsev, Tom Westerhout, Apoorv Tiwari, Kenny Choo, Ao Chen, Mark H Fischer, Giuseppe Carleo, and Titus Neupert. Broken-symmetry ground states of the heisenberg model on the pyrochlore lattice. *arXiv preprint arXiv:2101.08787*, 2021.
- [10] Kurt Hornik, Maxwell Stinchcombe, and Halbert White. Multilayer feedforward networks are universal approximators. *Neural networks*, 2(5):359–366, 1989.
- [11] Kenny Choo, Titus Neupert, and Giuseppe Carleo. Two-dimensional frustrated j_1-j_2 model studied with neural network quantum states. *Physical Review B*, 100(12):125124, 2019.
- [12] Francesco Ferrari, Federico Becca, and Juan Carrasquilla. Neural gutzwiller-projected variational wave functions. *Physical Review B*, 100(12):125131, 2019.
- [13] Di Luo, Zhuo Chen, Kaiwen Hu, Zhizhen Zhao, Vera Mikyoung Hur, and Bryan K Clark. Gauge invariant autoregressive neural networks for quantum lattice models. *arXiv preprint arXiv:2101.07243*, 2021.
- [14] Di Luo, Giuseppe Carleo, Bryan K Clark, and James Stokes. Gauge equivariant neural networks for quantum lattice gauge theories. *arXiv preprint arXiv:2012.05232*, 2020.
- [15] Tom Vieijra, Corneel Casert, Jannes Nys, Wesley De Neve, Jutho Haegeman, Jan Ryckebusch, and Frank Verstraete. Restricted boltzmann machines for quantum states with non-abelian or anyonic symmetries. *Physical review letters*, 124(9):097201, 2020.
- [16] Peter Broecker, Juan Carrasquilla, Roger G Melko, and Simon Trebst. Machine learning quantum phases of matter beyond the fermion sign problem. *Scientific reports*, 7(1):1–10, 2017.
- [17] Kaiming He, Xiangyu Zhang, Shaoqing Ren, and Jian Sun. Deep residual learning for image recognition. In *Proceedings of the IEEE conference on computer vision and pattern recognition*, pages 770–778, 2016.
- [18] Christian Szegedy, Sergey Ioffe, Vincent Vanhoucke, and Alexander Alemi. Inception-v4, inception-resnet and the impact of residual connections on learning. In *Proceedings of the AAAI Conference on Artificial Intelligence*, volume 31, 2017.
- [19] Taco Cohen, Maurice Weiler, Berkay Kicanaoglu, and Max Welling. Gauge equivariant convolutional networks and the icosahedral cnn. In *International Conference on Machine Learning*, pages 1321–1330. PMLR, 2019.
- [20] Sander Dieleman, Jeffrey De Fauw, and Koray Kavukcuoglu. Exploiting cyclic symmetry in convolutional neural networks. In *International conference on machine learning*, pages 1889–1898. PMLR, 2016.
- [21] Taco S Cohen, Mario Geiger, Jonas Köhler, and Max Welling. Spherical cnns. *arXiv preprint arXiv:1801.10130*, 2018.
- [22] Manzil Zaheer, Satwik Kottur, Siamak Ravanbakhsh, Barnabas Poczos, Ruslan Salakhutdinov, and Alexander Smola. Deep sets. *arXiv preprint arXiv:1703.06114*, 2017.
- [23] Kenny Choo, Giuseppe Carleo, Nicolas Regnault, and Titus Neupert. Symmetries and many-body excitations with neural-network quantum states. *Physical review letters*, 121(16):167204, 2018.
- [24] Yusuke Nomura. Helping restricted boltzmann machine with quantum-state representation by restoring symmetry. *arXiv preprint arXiv:2009.14777*, 2020.
- [25] Andrew M Pitts. *Nominal sets: Names and symmetry in computer science*, volume 57. Cambridge University Press, 2013.
- [26] Günter Klambauer, Thomas Unterthiner, Andreas Mayr, and Sepp Hochreiter. Self-normalizing neural networks. *arXiv preprint arXiv:1706.02515*, 2017.
- [27] Yasir Iqbal, Wen-Jun Hu, Ronny Thomale, Didier Poilblanc, and Federico Becca. Spin liquid nature in the heisenberg j_1-j_2 triangular antiferromagnet. *Physical Review B*, 93(14):144411, 2016.
- [28] B Bernu, P Lecheminant, C Lhuillier, and L Pierre. Exact spectra, spin susceptibilities, and order parameter of the quantum heisenberg antiferromagnet on the triangular lattice. *Physical Review B*, 50(14):10048, 1994.
- [29] Sandro Sorella. Generalized lanczos algorithm for variational quantum monte carlo. *Physical Review B*, 64(2):024512, 2001.
- [30] Ryuji Kaneko, Satoshi Morita, and Masatoshi Imada. Gapless spin-liquid phase in an extended spin 1/2 triangular heisenberg model. *Journal of the Physical Society of Japan*, 83(9):093707, 2014.
- [31] Fabio Mezzacapo and J Ignacio Cirac. Ground-state properties of the spin-antiferromagnetic heisenberg model on the triangular lattice: a variational study based on entangled-plaquette states. *New Journal of Physics*, 12(10):103039, 2010.
- [32] Sashank J Reddi, Satyen Kale, and Sanjiv Kumar. On the convergence of adam and beyond. *arXiv preprint arXiv:1904.09237*, 2019.
- [33] Diederik P Kingma and Jimmy Ba. Adam: A method for stochastic optimization. *arXiv preprint arXiv:1412.6980*, 2014.
- [34] Nikita Kitaev, Lukasz Kaiser, and Anselm Levskaya.

- Reformer: The efficient transformer. *arXiv preprint arXiv:2001.04451*, 2020.
- [35] William Fedus, Barret Zoph, and Noam Shazeer. Switch transformers: Scaling to trillion parameter models with simple and efficient sparsity. *arXiv preprint arXiv:2101.03961*, 2021.
- [36] François Chollet. Xception: Deep learning with depthwise separable convolutions. In *Proceedings of the IEEE conference on computer vision and pattern recognition*, pages 1251–1258, 2017.
- [37] Ashish Vaswani, Noam Shazeer, Niki Parmar, Jakob Uszkoreit, Llion Jones, Aidan N Gomez, Łukasz Kaiser, and Illia Polosukhin. Attention is all you need. *arXiv preprint arXiv:1706.03762*, 2017.
- [38] David Romero, Erik Bekkers, Jakub Tomczak, and Mark Hoogendoorn. Attentive group equivariant convolutional networks. In *International Conference on Machine Learning*, pages 8188–8199. PMLR, 2020.
- [39] Li Yang, Wenjun Hu, and Li Li. Scalable variational monte carlo with graph neural ansatz. *arXiv preprint arXiv:2011.12453*, 2020.
- [40] David Pfau, James S Spencer, Alexander GDG Matthews, and W Matthew C Foulkes. Ab initio solution of the many-electron schrödinger equation with deep neural networks. *Physical Review Research*, 2(3):033429, 2020.
- [41] Giuseppe Carleo, Kenny Choo, Damian Hofmann, James ET Smith, Tom Westerhout, Fabien Alet, Emily J Davis, Stavros Efthymiou, Ivan Glasser, Sheng-Hsuan Lin, et al. Netket: A machine learning toolkit for many-body quantum systems. *SoftwareX*, 10:100311, 2019.
- [42] Attila Szabó and Claudio Castelnovo. Neural network wave functions and the sign problem. *Physical Review Research*, 2(3):033075, 2020.